ELECTRONICS FOR PRECISION ALIGNMENT OF THE GEM MUON SYSTEM

Joseph A. Paradiso
MIT Media Laboratory, 20 Ames St., Cambridge, MA., 02139

Daniel R. Marlow
Joseph Henry Laboratories, Princeton University, Princeton, NJ 08544

ABSTRACT

In order to perform a precision measurement of high p_t muon tracks, the mechanical alignment of the GEM muon drift chambers was to be monitored with extraordinary accuracy; i.e., the sagitta error induced into muon tracks by superlayer misalignments must be held within 25 microns RMS across spans of several meters. As there are thousands of chambers to monitor, the resulting system must be simple, reliable, and inexpensive. The GEM muon group has explored two types of alignment sensors for this application, namely three-point Video Straightness Monitors and stretched wires with mini-strip pickup pads and axial pickup rings. This paper gives an overview of these systems and describes their associated electronics.

1) Introduction

The GEM muon system[1] is designed to achieve high momentum resolution by precisely measuring muon trajectories at three equidistant superlayers separated by a long lever arm in a large magnetized volume. In order to retain the desired precision at high momentum (i.e., $\Delta p_t/p_t \approx 5\%$ for the barrel detector at p_t = 500 GeV/c), the muon system must determine the net 3-point sagitta of a muon track to σ = 55 μm in the bending plane, as depicted in Fig. 1. After accounting[1] for the chamber resolution, mechanical tolerances, and multiple scattering, an error of σ=25 μm was allotted to the determination of superlayer alignment, as projected onto the sagitta (bending) coordinate.

Rather than placing the chambers precisely and requiring a muon support structure to hold this level of accuracy, the superlayer misalignment was to have been periodically monitored, and the resulting measurements used to update the muon chamber positions during track reconstruction. In its final stages, the GEM muon detector assumed an axial/projective alignment geometry[2,3], as depicted for a barrel module in Fig. 1 (this is a simplified schematic not showing chamber Lorentz tilt and overlap, etc.). Here, a set of multipoint axial monitors (i.e., stretched wires) is used in each superlayer to define straight lines across the separate muon chamber packages stacked along the beam direction, and 3-point optical projective monitors are used to measure and interpolate[4] the sagitta error between the three superlayers at the barrel edges (θ = 90° and 30°). Both axial and projective monitors are referenced to precision, stress-

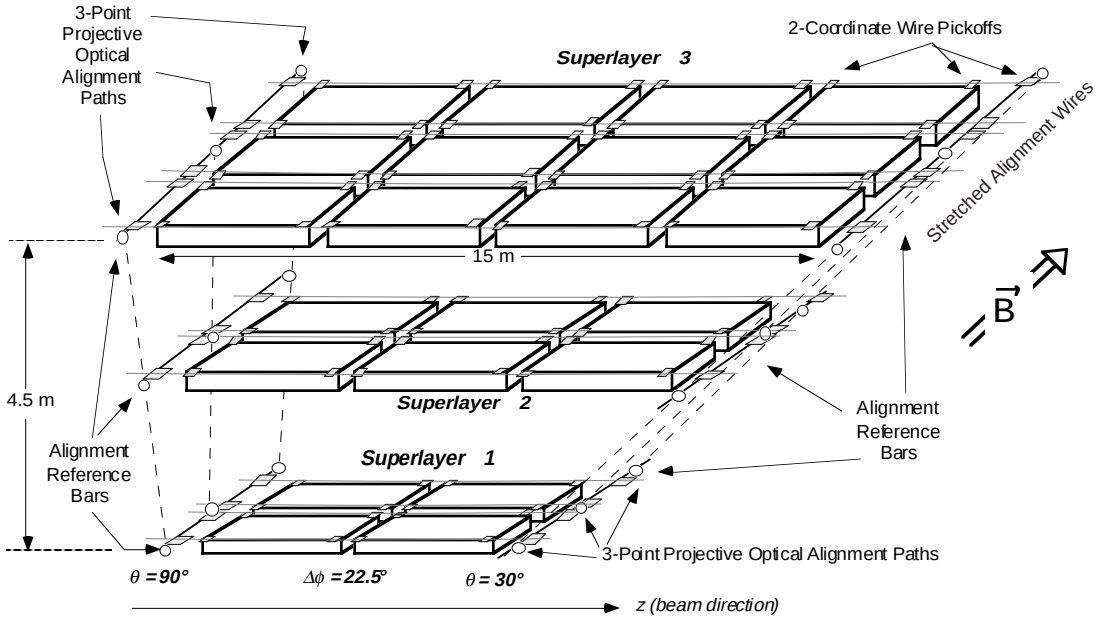

Figure 1: Axial/Projective alignment in the GEM barrel module

free, composite transfer plates ("Alignment Reference Bars" in Fig. 1), which provide a common interface between the interlayer and axial alignment systems. Simulations[5,6,7] have indicated that the 25 μm alignment goal can be obtained with 3-point interlayer monitors that resolve sagitta displacement to within σ=15 μm (across paths reaching 9 meters), and stretched wires (up to 15 meters long) that resolve sagitta displacement to within σ=10 μm and radial shifts (away from the beamline) to within σ=200 μm. In order to accomodate rapid assembly and potential structural drift, these monitors should operate over a dynamic range of 1 cm or more.

2) Wide-Range Optical Straightness Monitors

Three-point optical straightness monitors were first developed[8] for the L3 muon detector at LEP, where they were deployed as the RASNIK[9] system. These are simple devices composed of a light source, lens, and position-sensitive photodetector, as shown in Fig. 2. An image of a smooth-aperture, collimated source (i.e., LED) is projected onto a planar detector (i.e., quadrant photodiode) through a focusing lens. Displacements of the lens from the line between source and detector are measured as a shift in the illumination centroid at the photodiode. When precisely mounting[10] one component (LED, lens, detector) at each superlayer, an array of these devices can dynamically monitor the 3-point interlayer sagitta error, as diagrammed in Fig. 1.

With the lens at the midpoint, these devices have an implicit gain of two in the sagitta measurement; the offset read at the detector is twice the 3-point sagitta error. The measured displacement is relatively insensitive to rotations of the lens and LED (provided it exhibits a symmetric illumination profile) about their optical axes. The LED is modulated by a low-frequency carrier, and synchronously sampled to effectively place a very narrow filter around the transmit frequency, minimizing the effects of any ambient light background (this principle is discussed further in Sec. 3). Electronics following the block diagram in Fig. 2 have been built for these devices by NIKHEF[9] for L3 and Harvard[11] for SDC.

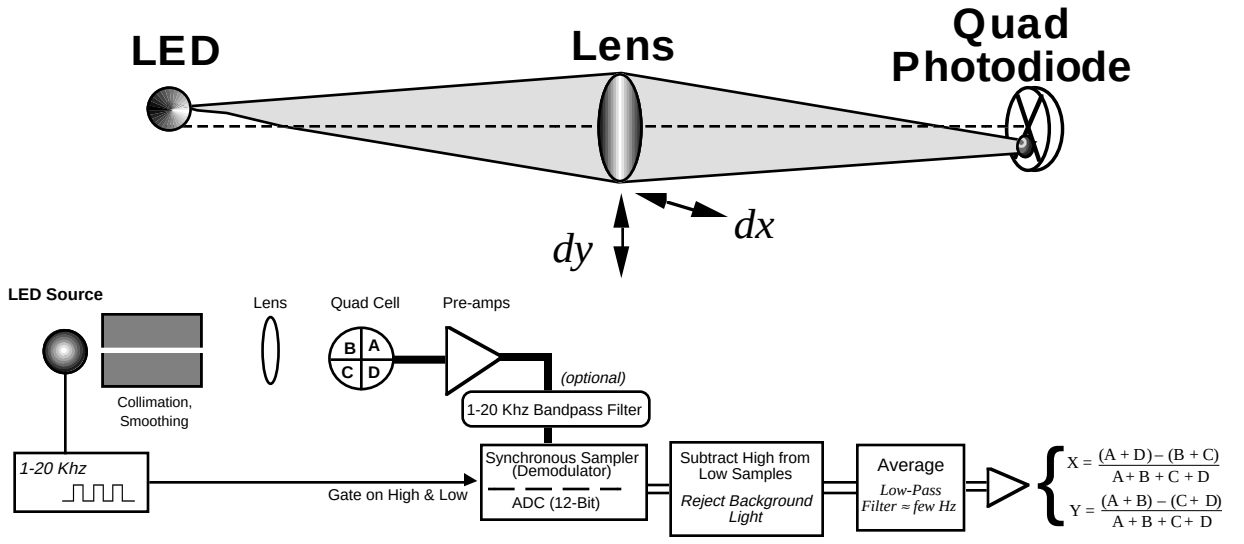

Figure 2: Standard 3-point straightness monitor (SLM) and associated readout electronics

Although simple LED/Lens/Quad-cell systems such as depicted in Fig. 2 are proven to provide high accuracy in deployed detector systems (i.e., below 5 μm[9,12]) at minimal cost, their useful measurement range doesn't generally extend beyond 1-2 mm. The range of these alignment systems may be increased by replacing the quad-cell with a continuous lateral-effect photodiode[13] or by employing a wide-area diffuser over the LED and using a larger quadrant diode[14]. Another possibility[10] is to use a dense array of multiple LED's with overlapping linear range at the quad cell, and illuminate each in succession. These techniques, however, can appreciably increase the hardware complication and expense, plus potentially degrade the alignment resolution beyond the 15 μm limit.

In the years since L3 was installed, dramatic progress has occurred in video technology and image processing. These advances have been exploited at GEM, evolving the simple SLM of Fig. 2 into the Video Straightness Monitor (VSM)[15] of Fig. 3. Here, instead of putting a quadrant photodiode at the focal plane, an imaging array is placed there to collect much more information (i.e., tens of thousands of pixels, as opposed to only four). Likewise, instead of imaging a simple spot, as in Fig. 2, we project a complicated pattern.

This approach has two major advantages. First, since the image is projected and detected over a full frame with many pixels, there is much more tolerance to local defects in the projected image and the focal plane array (this relieves much of the tedious calibration and component selection needed in SLM systems). Second, the operating range is greatly increased. Only a portion of the projected image need be seen by the sensitive array; if it is unambiguous, a correlation with the mask template will determine the offset between the array and the global image.

Recent advances in imaging technology and related microelectronics have dramatically reduced the cost and size of solid-state video cameras. Highly integrated, miniature monochrome cameras are now available, costing below $100 in moderate quantities. They are self-contained, in that they typically require only 7-16 V of power and will output composite RS-170 video onto a 75 Ω cable. Several of these devices have been tested[16] for VSM

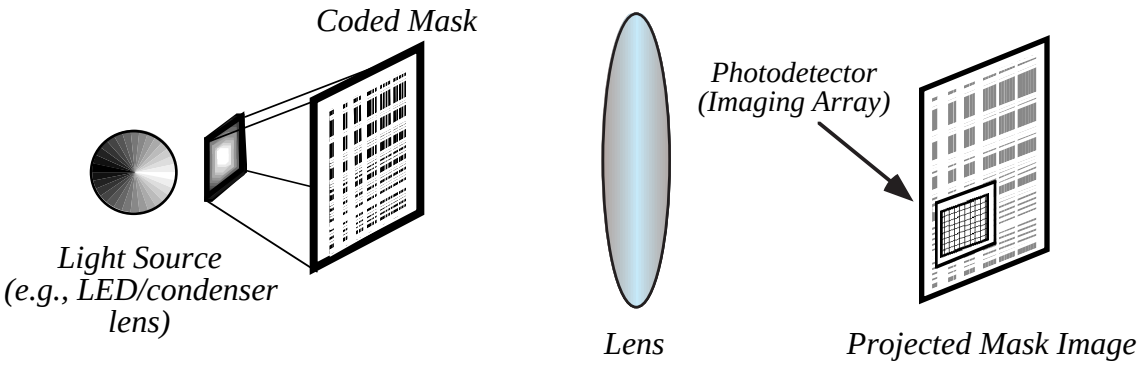

Figure 3: Video Straightness Monitor (VSM) scheme

Figure 4: Miniature monochrome cameras for VSM application from Chinon (left) and VVL (right)

application. Two are shown in Fig. 4, both compared in size to a US quarter. At left is the CX-103 from Chinon corporation, measuring 44 x 46 mm, and incorporating a 1/3" MOS photodiode sensor with 324 x 246 elements (operating down to 2 Lux @ F1.8), full electronic shutter, AGC, and RS-170 formatting on-card. This unit, however, still has several discrete IC's to clock the MOS sensor and process the video. At right, in contrast, is the "Peach" video camera[17] (the lens assembly is swiveled up to view the internal circuitry) from VVL corporation in Edinburgh, Scotland. This device has the sensor (operating down to 5 Lux @ F1.8) plus all video formatting and signal processing integrated onto the same CMOS monolithic. It contains a 1/2" array of 312 x 287 pixels, and produces standard CCIR video; the video may also be output synchronously with an external clock. As of last year, the Peach chip (ASIS-1011-B) was available for under £30. in quantities of over 200. This technology has an exploding future in many emerging commercial media applications, and is still being aggressively developed. VVL is now producing superior chips with a 512 x 512 matrix, and Chinon has announced the CX-060, which likewise integrates all video processing onto a single chip (this features a low-noise 1/3" CCD array with 512 x 496 pixels, RS-170 formatting, and operates down to 0.5 Lux @ F1.8).

These devices must perform in the GEM magnetic field, which can reach the neighborhood of 2 Tesla in the muon region. The CX-103 (left in Fig. 4) fails at fields beyond 1 KG, because of an inductive DC-DC converter used on the card. The monolithic devices, on the other hand, have no such problem; i.e., the VVL chip has been used in very high fields to

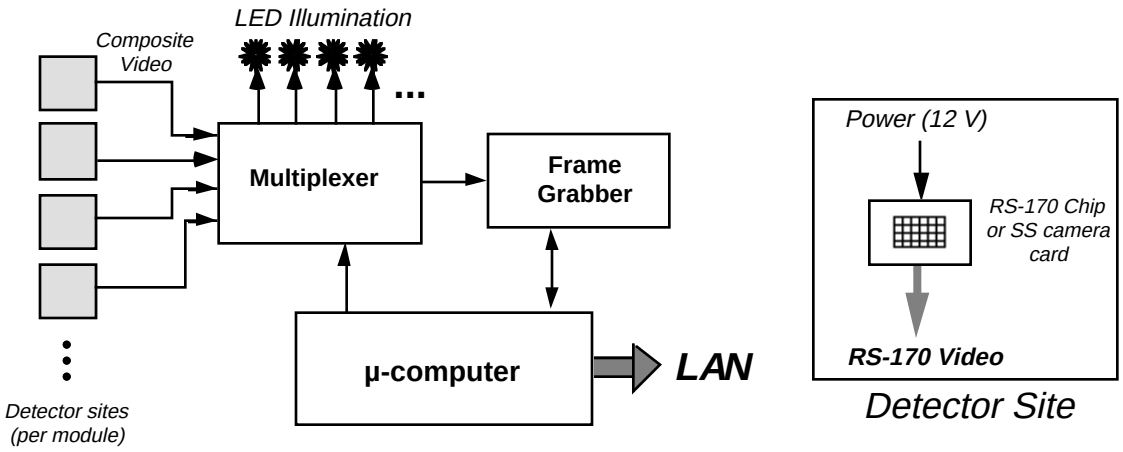

Figure 5: Multiplexed application of a system with several VSM sites

observe patients in magnetic resonance imagers. It is anticipated that these devices will tolerate the anticipated radiation dose in the muon region; if a Charge Injection Device (CID) is used as an imaging array, however, the VSM concept can be used in worse radiation environments[18].

As depicted in Fig. 5, the implementation of such a system at a large detector such as GEM is very simple, potentially even more straightforward than an equivalent SLM deployment. All video outputs in a segment of the detector are routed to a multiplexer; if the cameras can also be powered through the video coax, only one cable is needed per camera site. When acquiring data, the supervisory processor addresses the multiplexer for the appropriate camera and activates the corresponding LED illuminator. Granted, we lose the ability to easily do synchronous detection here, but this is much more important for SLM's, where extraneous light can severely affect the centroid balance. As shown in tests[10], the mask is well illuminated when using a combination of LED and condenser lens (which collimates the light like a flashlight beam), with a short (i.e., 10 cm) tube placed around the imaging array to exclude extraneous light.

A series of frames is then acquired at each camera site and averaged to attenuate transient thermal disturbance (tests in the laboratory[10] have indicated that averaging frames at 1 Hz for 15 seconds is normally sufficient), whereupon a simple correlation analysis fits the detected mask offsets to its generated template, producing the required alignment measurements.

Because of jitter in phase-lock loop circuitry, standard asynchronous consumer-quality frame grabbers typically are able to resolve no better than 20% of the pixel pitch[19] after they warm up, thus producing under 4 microns of error with a typical imaging array, which is adequate for the intended application at GEM. Synchronous grabbers (with one memory location per pixel) are accurate to better than 3% of the pixel pitch[19], but are not needed at GEM, sparing their additional expense and hardware complication.

The VSM image processing requirements are minimal when using an efficient mask coding and analysis procedure. Fig. 6 (left) shows the mask that was used for prototype tests; it is a coincident 2-dimensional barcode (with vertical bars running black-on-white, and horizontal bars running white-on-black), and was defined entirely in PostScript, then printed on a Linotype and reduced to a square 2.4 cm on a side. A $^1/_3$" array thus sees 6% of the mask area (assuming a 1:1 projection); the barcode is designed such that at least one full digit (sandwiched between thick bars) can always be read anywhere in this field, disambiguating the camera offset in the projected image.

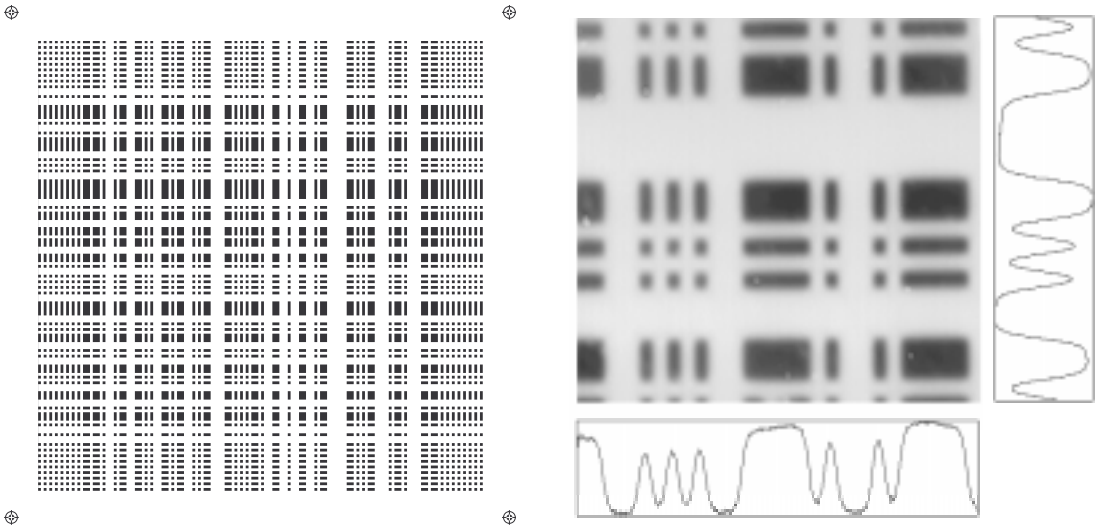

Figure 6: 2-Dimensional coincident barcode mask (left) and captured VSM frame (right)

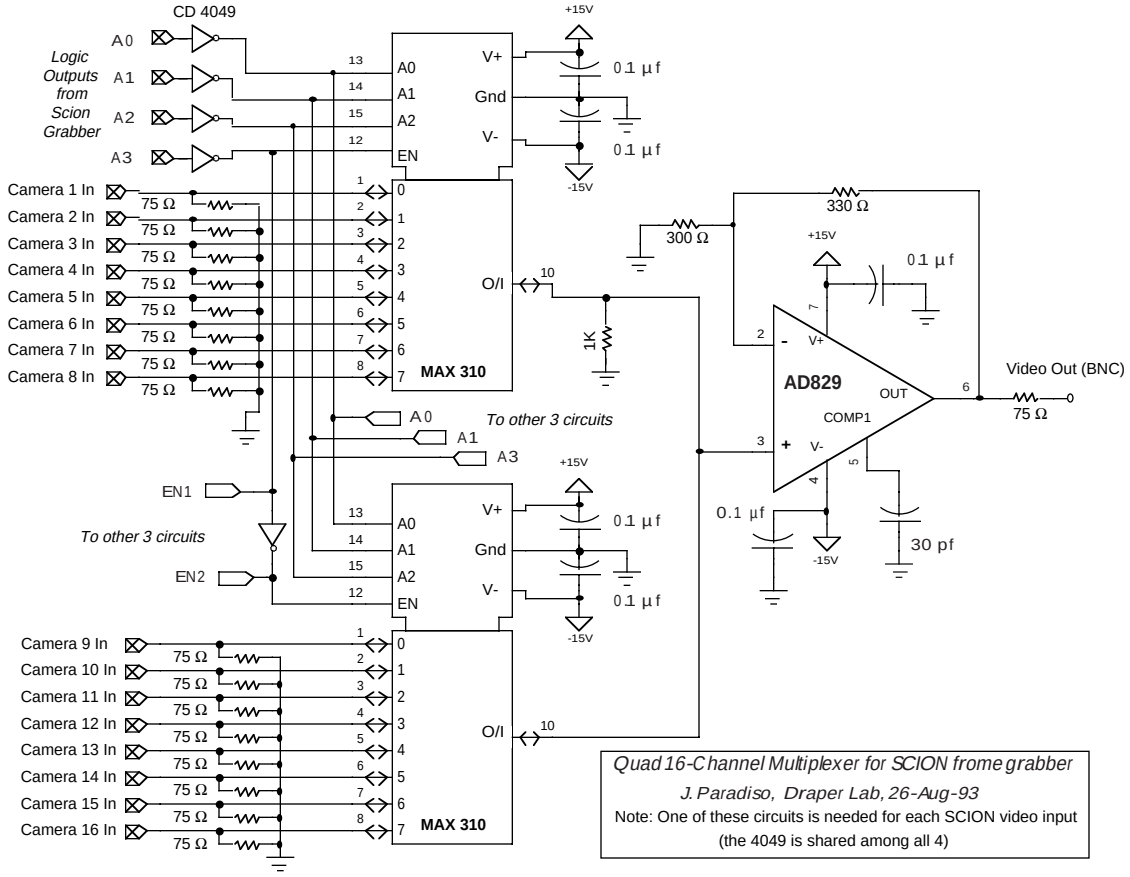

Figure 7: 16-Channel video multiplexer designed for the GEM Alignment Test Stand

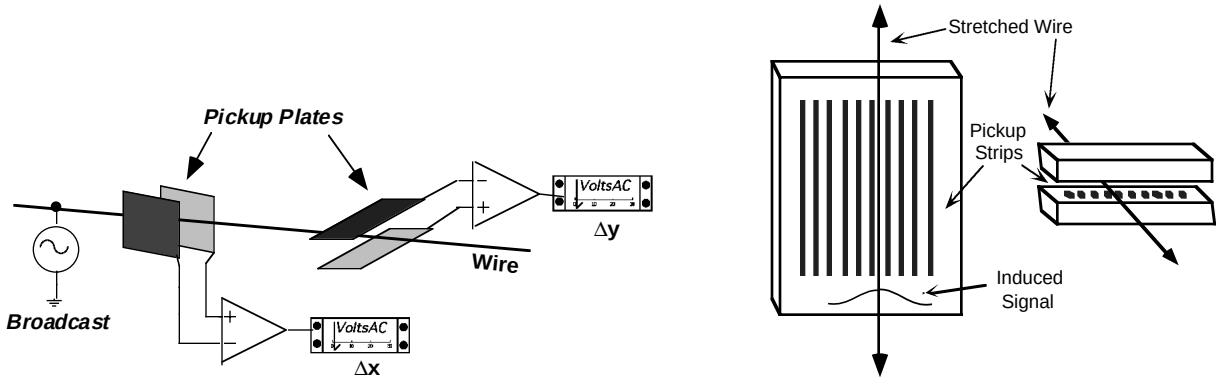

Figure 8: Conventional (left) and mini-strip (right) pickups for stretched wire alignment

An actual frame is displayed at right in Fig. 6, as captured in the VSM prototype across an 8 meter baseline with a ø=42 mm lens at midpoint. The barcode can be well discerned; the small bars are 120 μm thick. The plots at bottom and right of this frame show horizontal (x) and vertical (y) projections (i.e., all pixels are summed into one row and one column), in which a segment of the x and y barcodes can be clearly seen. A simple analysis[20] reads the barcode fragments on these two projections, identifies the features, then centroids the bars and matches these values (in pixels) to their corresponding locations on the template (in mm) with a linear least-squares fit, producing very accurate alignment offsets. Performing such a simple analysis on the (x,y) frame projections breaks a complicated 2D cross-correlation operation into two very simple 1D linear fits, enabling the software to execute very quickly, potentially surpassing the 30 Hz frame rate with a simple processor.

Several tests have been run on VSM prototypes at Draper[10,16,20] and NIKHEF[21]. These have demonstrated very high resolution of straight-line misalignment spanning wide dynamic range across long optical paths (i.e., 2 μm RMS over 12 mm of lens deflection and across an 8-meter mask to camera baseline), which well surpasses the GEM goals.

The Draper tests acquired and averaged a single channel of video via a Data Translation DT2861 frame grabber in an IBM PC. A simple 16-1 video multiplexer was designed (Fig. 7) for implementing the system of Fig. 5 at the proposed GEM Alignment Test Stand[22]. Here, real-time frame acquisition and analysis would based entirely around a Macintosh using a single SCION LG-3 frame grabber. This NuBus card inputs 4 channels of video, and contains a 4-bit digital output register, thus can directly address up to 64 VSM channels via the circuit of Fig. 7.

3) Stretched Wire Axial Alignment

An ideal stretched wire forms a perfect straight-line reference for multi-point alignment, and is well suited to defining the superlayer planes of Fig. 1. Inexpensive proximity pickups can be placed anywhere along the wire (i.e., at the chamber edges and midway along the perimeter to also monitor chamber deformation). Of course, a wire is a mechanical construct, which must be strung between endpoints, monitored to track sag, and kept away from vibrational excitation and breakage. New light, strong, composite wires are now becoming available that reduce the sag and vibrational problems (such as Silicon Carbide[23]), making a set of stretched wires a leading option for the GEM axial alignment.

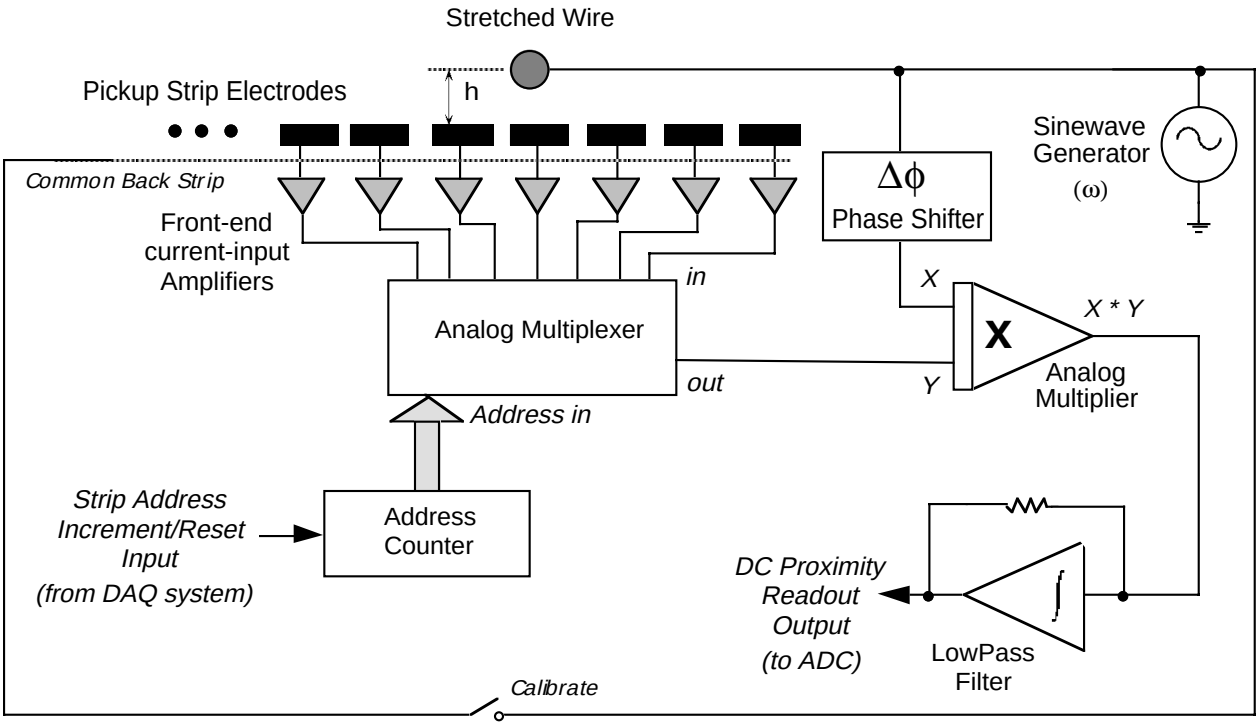

Figure 9: Readout of mini-strip stretched wire pickups

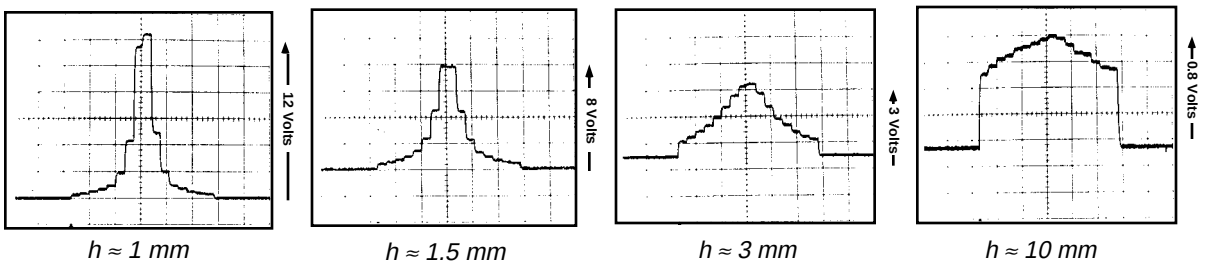

Figure 10: Mini-strip signals for wire at various heights (h) from strip board

Fig. 8 depicts the standard method of determining the position of a sensor relative to a conducting wire; i.e., the wire forms a differential capacitor between a set of parallel plates. As the wire approaches one plate or the other, the induced signal increases on the closer plate (and decreases on the opposite plate), thus the difference between plate currents is a function of wire displacement (the wire position can also be determined optically[24], but this generally has very limited dynamic range). An accurate measurement across a pair of plates thus relies on very precise electrical and mechanical calibration of the readout components.

An alternative to this conventional scheme, shown at right in Fig. 8, was proposed[3] to relax these requirements, much in the spirit of the SLM to VSM evolution described earlier (i.e., the VSM collects many thousands of pixels, vs. the 4 channels monitored by the quadrant detector). Here, we pixellate the pickup electrodes into a series of strips at a 1 mm pitch; the wire-induced signals on these strips are digitized, allowing the footprint of the wire to be effectively "imaged" at the pickup plate, and a precise centroid determined, as sketched in Fig. 8.

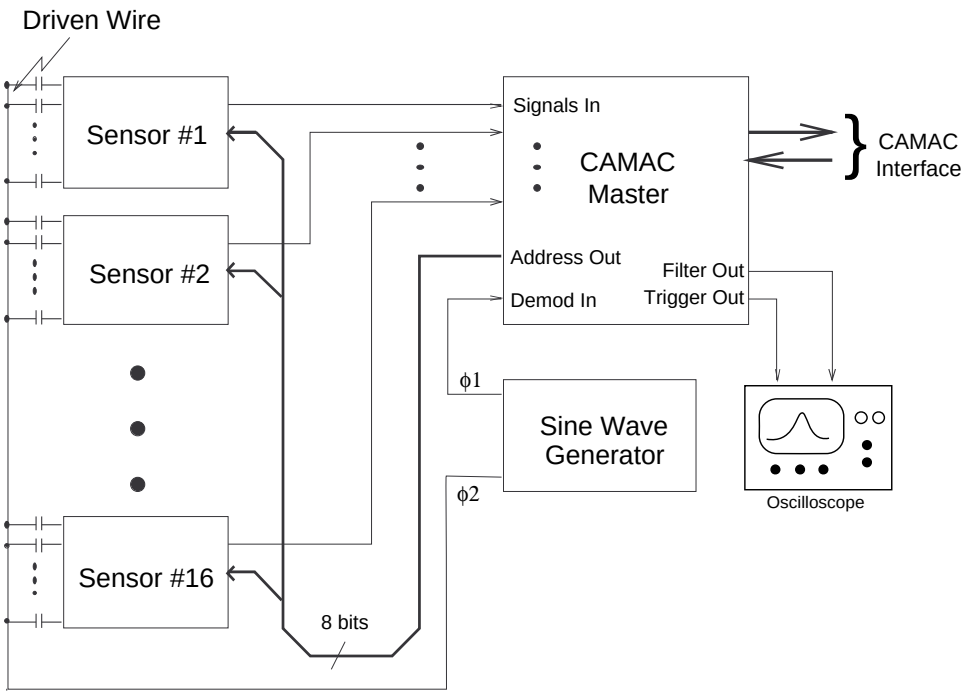

Figure 11: Block diagram for a CAMAC-based system to readout a collection of mini-strip boards

The readout electronics used with the mini-strips is diagrammed in Fig. 9, and detailed in Ref. [7]. A synchronous detection scheme is employed to measure the signal coupled from the wire, similar to that implemented in Fig. 2 for the SLM's. An analog multiplier demodulates the pickup signal with the same waveform applied to the wire; the detected signal then has components at DC and twice the transmitted frequency (ω). A low-pass filter selects the DC component, simultaneously filtering out most out-of-band interference, thereby providing a proximity detection with very low extraneous noise. Although an analog switch can also be used here for demodulation, excellent performance has been obtained with a low-cost analog multiplier (AD633), which is shared across all strip channels.

The front-end amplifiers are configured as current-to-voltage converters (i.e., an AD713 op-amp with a 200K - 1M resistor in feedback), which provide a very low impedance at the strips, making the electric field configuration (thus induced signal distribution) a well-defined cylindrical dipole[3,23]. As the front-end measures the current flowing across the small wire/strip capacitance, it acts as a hard differentiator, hence the strip signals are 90° out of phase with the wire drive (in the absence of front-end rolloff), requiring a phase shifter at the multiplier ($\Delta\phi$ in Fig. 9), which was realized as an all-pass filter in the prototype circuit. The wire drive runs between 10-30 V p-p, and the transmit frequency (ω) is set between 20-100 kHz; this gives plenty of coupling strength, but is sufficiently low to avoid major roll-off at the generic op-amps used in the front-end. The cutoff frequency of the low-pass filter at the multiplier output is set circa 300 Hz to filter out the most extraneous pickup and still allow rapid cycling through the multiplexer and transmission of the wire dynamics (all below 50 Hz), which can be purposefully excited to measure wire sag[25].

Although the mini-strip segmentation considerably relaxes the requirements on pickup gain uniformity, the front-end circuits can be precisely calibrated by driving a backing strip and coupling a common signal into all pickups, as sketched in Fig. 9.

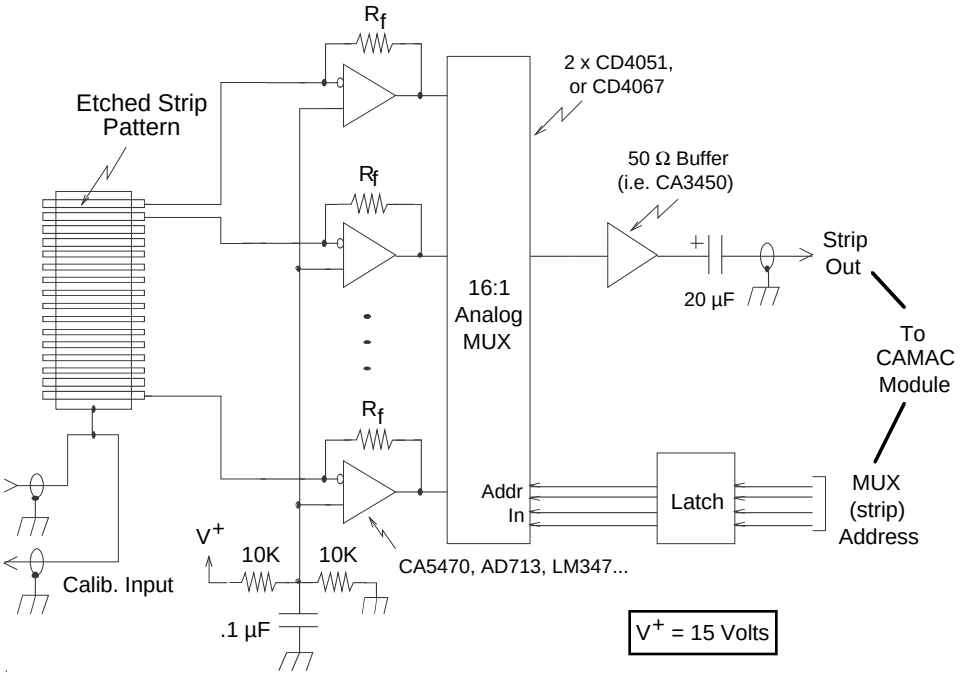

Figure 12: Design of mini-strip sensor boards

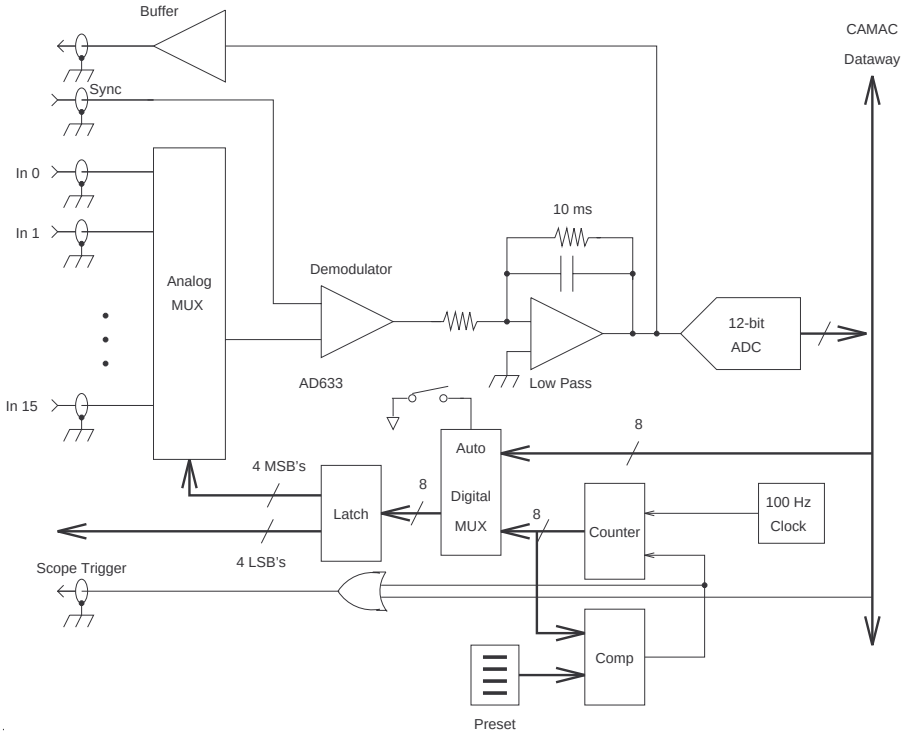

Figure 13: Design of CAMAC master module

Command	Response	Q=1 if
F(0)	Read MUX address	
F(1)	Read A/D	A/D data valid
F(2)	Read MUX address & clear LAM	
F(3)	Read A/D & clear LAM	A/D data valid
F(8)	Test LAM	LAM set
F(16)	Set MUX address	
F(25)	Increment MUX address	
F(28)	Start A/D conv., set LAM on A/D data valid	
F(29)	Issue scope trigger	

Figure 14: CAMAC commands implemented in stretched-wire readout module

Fig. 10 shows the demodulated outputs across a set of 16 strips for increasing wire distances from the strip board. The circuit of Fig. 9 was used, with the multiplexer toggling through sequential strips (thus the steps on the horizontal axis of these plots denote the strip number). The position of the wire can be clearly determined across the strips, especially in the case at left, with the wire only 1 mm above the strip board. Although the distribution widens as the wire is elevated and the field lines spread out to more strips, this centroid remains well determined. Since the width is strongly correlated with the height of the wire above the strip board (and only weakly correlated with strip board rotation)[3,23], the distance of the wire from the strip plane can also be determined.

A set of tests has been performed[23] at MIT to determine the precision of these measurements. For the wire displaced up to 1 cm over the strip board, the wire position could be determined to within $\sigma<3$ μm across the strips (sagitta direction in GEM; Fig. 1) and $\sigma<100$ μm above the strip board (radial direction in GEM), thus this technique can deliver the accuracy needed for a GEM axial monitor, as specified in Sec. 1.

In order to test the wire readout at many points across long wires (and thereby monitor wire sag and associated effects), several pickup boards need to be read out, hence a CAMAC system (Fig. 11) has been designed along the lines of the prototype (Fig. 9) and fabricated at Princeton[26] to fulfill this need. The "Sensor" units of Fig. 11 are depicted in Fig. 12; these consist of the mini-strip cards (sixteen 5 cm-long strips at 1 mm pitch, as used in tests[23], together with common calibration strip) followed closely by shielded front-end amplifiers in close proximity, which feed a 16-1 CMOS analog multiplexer that drives a cable to the CAMAC module. The strip output that is selected by the multiplexer is determined by a 4-bit parallel address bus, which is produced in the CAMAC module and daisy-chained to all sensor boards.

The CAMAC module is diagrammed in Fig. 13. Here, we see that each strip has an 8-bit address; the 4 LSB's are routed to all sensor boards to select the strip, as described above, and the 4 MSB's address a multiplexer in the CAMAC module that selects the signal coming from a particular strip board for demodulation, filtering, and 12-bit digitization. The 8-bit address can be set directly from CAMAC commands or through an internal counter, which cycles across all strips in a board and produces a synchronous trigger, allowing the sequential strip signals to be viewed directly on an oscilloscope (Fig. 11), producing displays similar to those of Fig. 10 for

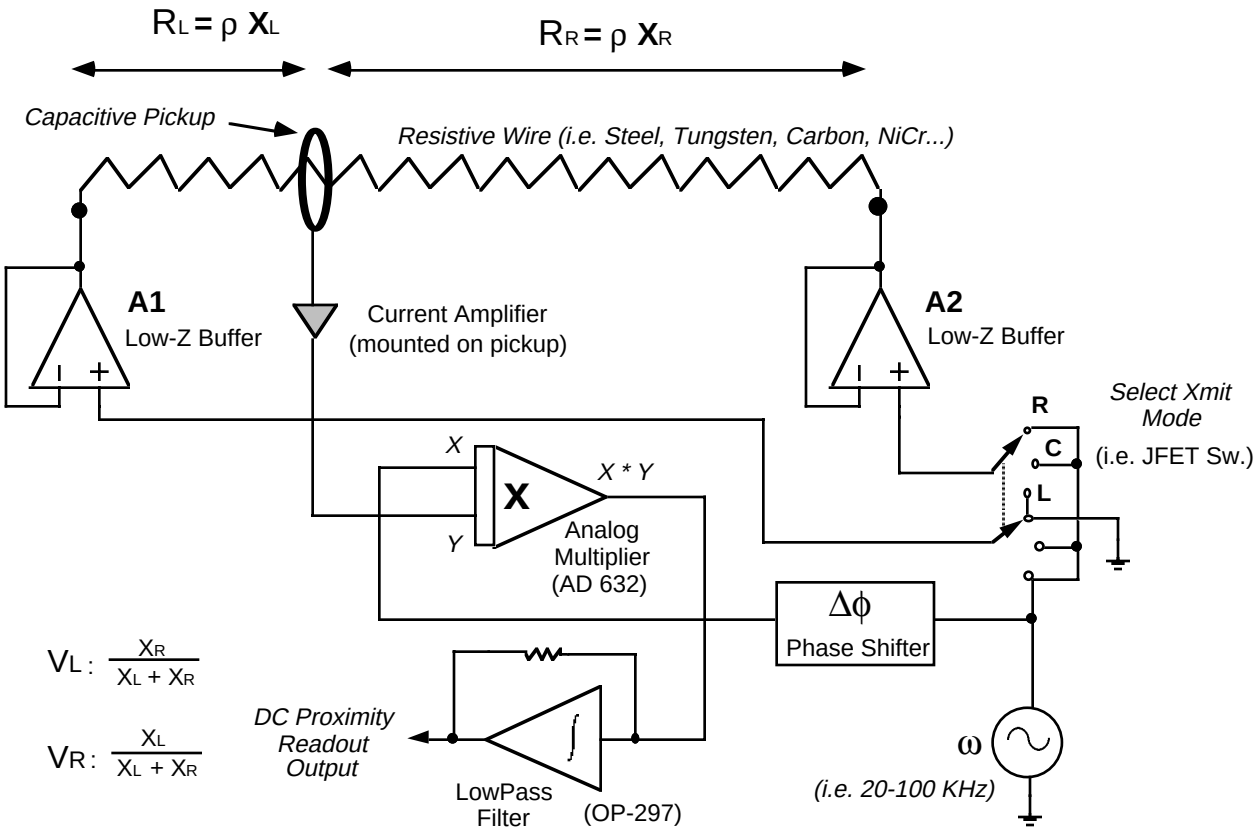

Figure 15: Setup for measuring axial position along stretched resistive wire

diagnostic purposes. The list of CAMAC commands which this unit accepts is summarized in Fig. 14.

The oscillator in Fig. 11 was also to be implemented eventually in CAMAC, with programmable frequency, quadrature outputs ($\phi 1$, $\phi 2$), and addressable wire drivers, such that a set of alignment wires will transmit only when data is being taken. In addition, this unit would feature programmable calibration outputs to drive the backing strips on the sensor boards.

The mini-strips measure only the coordinates in the plane normal to the wire. The GEM muon system would also benefit from a coarser (i.e., mm-level) measurement of the axial coordinate along the wire, particularly during survey and installation. Fig. 15 shows a method of detecting the axial position of a pickup along a stretched wire. A resistive wire is used as a voltage divider, and a shielded cylindrical capacitive pickup performs the function of a potentiometer wiper; i.e., provides a very high impedance (typically, $C < 1$ pf) noncontact ($r > 1$ cm) tap into the local wire signal. The pickup current is ideally proportional to the driving voltage and capacitive coupling, weighted by the fractional distance along the wire from the location of the pickup to the grounded end. By driving first one end of the wire and grounding the other, then vice-versa (i.e., flipping the switch in Fig. 15 between R and L), and taking the sum over difference of the measured voltages, the variable gain factors divide out, leaving a clean measurement of the fractional displacement along the wire.

Despite the fact that only mm-level precision is desired from this measurement, the wire may be many meters in length, entailing a wide dynamic range. As a result, the multiplier and

filter must be realized using low-drift components, as listed in Fig. 15. The nature of the wire is crucial; it should ideally be of uniform resistivity with a low temperature coefficient. The latter factor is answered by using a wire made of nichrome ($\Delta\rho/\rho = 0.0002/°C$) or EVENOHM® alloy[27] (used in wirewound resistors; $\Delta\rho/\rho = 0.000002/°C$), and the former addressed by using a superior grade of wire, or calibrating a the wire with an axial scan. Provided a uniform and stable resistive coating can be applied, the composite wires investigated for GEM (i.e., silicon carbide) can also be adapted for this application. The same wire can be used for mini-strip measurements by driving both ends in phase (the switch in Fig. 15 set to "C").

An axial wire readout system has been prototyped, and has demonstrated local (i.e., within a 10 cm neighborhood) position resolutions of 50-100 μm RMS on a tungsten wire up to 3.1 meters in length ($Z = 120\ \Omega$). When displacing away from the local region, defects in the low-grade wire that was used became significant; nonetheless, position resolutions of under 500 μm RMS were obtained across 1.5 meter spans. Further details on axial alignment (i.e., principles, electronics, test measurements) are given in Ref. [25].

4) Conclusions

Both the Video Straightness Monitors and mini-strip stretched wires produce improved, calibration-tolerant, position resolution over a wide dynamic range by employing an analogous principle: pixellating a formerly coarse measurement into a finer level of detail. The rapid advance of small integrated video cameras and image processing equipment has enabled the VSM's to be constructed economically, mainly from commercially-available devices; little custom electronics development was required. On the other hand, all electronics used for stretched wire readout have been developed within GEM, but are quite inexpensive (and can be heavily multiplexed), easily enabling the realization of multi-sensor stretched wire alignment systems. By separately driving each end of a resistive wire, an axial position measurement can also be obtained. Although these technologies were developed with the goals of the GEM muon system in mind, they are readily applicable to other high-energy physics detectors and accelerators; i.e., wherever a collection of mechanical components must be precisely aligned.

5) Acknowledgments

We thank and acknowledge Andrey Korytov of MIT/LNS for his collaboration on stretched wire alignment and Harry van der Graaf, of NIKHEF, Amsterdam for participating in VSM development. The optical advice of Jacques Govignon and Dave Goodwin from Draper Laboratory was also appreciated, as was the help of Dale Ross and Louis Osborne at MIT during the stretched wire tests. The collaboration with Neil Gershenfeld of the MIT Media Laboratory in designing cello and violin bow tracking systems was very useful when perfecting the synchronous readout for the stretched wire systems. Stan Chidzik and Dick Rabberman of Princeton are also thanked for their contributions in designing the PC board for CAMAC wire readout.

References:

[1] “GEM Technical Design Report,” Chapter 4, GEM-TN-93-262.

[2] Paradiso, J., "Some Alignment Concepts for the GEM Muon Array," GEM-TN-92-124, June, 1992.

[3] Korytov, A., "The Axial + Projective Alignment for Muon Chambers," GEM TN-93-302, March, 1993.

[4] Mitselmakher, G. and Ostapchuk, A., "New Approach to Muon System Alignment," GEM TN-92-202, October 1992.

[5] Mitselmakher, G. and Ostapchuk, A., "Alignment Requirements for the GEM Muon System", GEM TN-93-333, March, 1993.

[6] Paradiso, J., "Analysis of an Alignment Scheme for the GEM Muon Barrel," GEM-TN-92-150, October, 1992.

[7] Paradiso, J., "Synchronous Proximity Detection for Stretched-Wire Alignment Systems" GEM-TN-93-447, August, 1993.

[8] Toth, W. E., "Muon Detector Program; Prototype Octant Construction and Evaluation with Production Phase Recommendations", Draper Lab Report CSDL-R-1885, Oct. 1987.

[9] Duinker, P., et. al., "Some Methods for Testing and Optimizing Proportional Wire Chambers", *Nuc. Inst. and Methods*, A273 (1988), pg. 814-819.

[10] Paradiso, J., "Testing and Development of Extended Range Straightness Monitor Systems", GEM TN-93-331, May, 1994.

[11] Conceptual Design Report; Winerack Design of the SDC Barrel and Intermediate Muon Chambers, Section II-F, SDC-92-179, 1992.

[12] Ayer, F. et. al., "The Engineering Development of an Actively Controlled Precise Muon Chamber for the SDC Detector", *Proc. of the SSCIII Conference, New Orleans, LA*, March 1992.

[13] Govignon, J., Ayer, F., "Implementation of an Optical Fencepost for the Alignment of the SDC Muon System", SDC-92-393, Dec. 14, 1992.

[14] Post, W., "A Homogeneous Lightsource for RASNIK", NIKHEF-H report, July/August, 1992.

[15] Paradiso, J., "Application of Miniature Cameras in Video Straightness Monitor Systems", GEM-TN-94-608, June 1994.

[16] Paradiso, J., van der Graaf, H., "Wide Range, Precision, Three Point Alignment System", Patent application submitted, Draper Lab patent disclosure # CSDL 1398, May 1994.

[17] "CMOS Light-Sensor Process Makes Possible Low-Cost Smart Machine-Vision Systems", *Electronic Design*, Vol. 41, No. 12, June 10, 1993, pp. 29-32.

[18] Carta, R., CIDTEC, Liverpool, NY 13088, Personal Communication, 1993.

[19] Heckel, W., "Use of CCD Cameras for Digital Image Processing; Synchronization, Precision and Sources of Errors" (pp. 125-132), and Ge, R., "Linejitter detection of CCD Cameras" (pp. 239-246), Optical 3-D Measurement Techniques II, Herbert Wichmann Verlag GmbH, Karlsruhe, Germany, 1993.

[20] Paradiso, J., Goodwin, D., "Wide-Range Precision Alignment For The Gem Muon System", Proc. of the Third International Workshop on Accelerator Alignment, Annecy, France, Sept. 28 - Oct. 1, 1993.

[21] Dekker, H., et. al., "The RASNIK/CCD 3-Dimensional Alignment System", Proc. of the Third International Workshop on Accelerator Alignment, Annecy, France, Sept. 28 - Oct. 1, 1993.

[22] Wuest, C.R. et. al., "The GEM Detector Projective Alignment Simulation System", Proc. of the Third International Workshop on Accelerator Alignment, Annecy, France, Sept. 28 - Oct. 1, 1993.

[23] Korytov, A., Osborne, L., Paradiso, J., Rosenson, L. and Taylor, F., "Multi-Point Wide-Range Precision Alignment Technique for the GEM Detector", Nuclear Instruments and Methods in Physics Research, A343, pp. 428-434, 1994.

[24] Sawicki, R., Bliss, E., Griffith, L., "Precision Alignment Capabilities at LLNL," GEM-TN-93-339, March 30, 1992.

[25] Paradiso, J. "A Simple Technique for Measuring Axial Displacement in Stretched-Wire Alignment Systems", GEM-TN-94-607, May, 1994.

[26] Marlow, D., "Wire Alignment Readout Electronics; Conceptual Design", Princeton/GEM internal memo, August 2, 1993.

[27] Carpenter Technology Corporation, Carpenter Steel Division, datasheet for EVANOHM® Alloy R.